

Long-term sedimentary recycling of rare sulphur isotope anomalies

Christopher T. Reinhard^{1,2}, Noah J. Planavsky^{1,2} & Timothy W. Lyons²

The accumulation of substantial quantities of O₂ in the atmosphere has come to control the chemistry and ecological structure of Earth's surface. Non-mass-dependent (NMD) sulphur isotope anomalies in the rock record¹ are the central tool used to reconstruct the redox history of the early atmosphere. The generation and initial delivery of these anomalies to marine sediments requires low partial pressures of atmospheric O₂ (p_{O_2} ; refs 2, 3), and the disappearance of NMD anomalies from the rock record 2.32 billion years ago^{1,4} is thought to have signalled a departure from persistently low atmospheric oxygen levels (less than about 10⁻⁵ times the present atmospheric level) during approximately the first two billion years of Earth's history. Here we present a model study designed to describe the long-term surface recycling of crustal NMD anomalies, and show that the record of this geochemical signal is likely to display a 'crustal memory effect' following increases in atmospheric p_{O_2} above this threshold. Once NMD anomalies have been buried in the upper crust they are extremely resistant to removal, and can be erased only through successive cycles of weathering, dilution and burial on an oxygenated Earth surface. This recycling results in the residual incorporation of NMD anomalies into the sedimentary record long after synchronous atmospheric generation of the isotopic signal has ceased, with dynamic and measurable signals probably surviving for as long as 10–100 million years subsequent to an increase in atmospheric p_{O_2} to more than 10⁻⁵ times the present atmospheric level. Our results can reconcile geochemical evidence for oxygen production and transient accumulation with the maintenance of NMD anomalies on the early Earth^{5–8}, and suggest that future work should investigate the notion that temporally continuous generation of new NMD sulphur isotope anomalies in the atmosphere was likely to have ceased long before their ultimate disappearance from the rock record.

One of the most important recent advances in studies of Earth's early atmospheric chemistry has been the demonstration that NMD sulphur isotope anomalies, often of very large magnitude, are preserved in sedimentary sulphide and sulphate minerals more than ~2.32 Gyr old^{1,4}. The generation and preservation of these anomalies is generally considered to require active and widespread tropospheric photochemistry involving SO₂ dissociation at short wavelengths, which in turn implies minimal ozone column depth²; a strongly reducing atmosphere, such that multiple exit channels for sulphur at different redox states can be maintained^{3,9}; and minimal metabolic overprinting of atmospherically derived isotope anomalies within marine environments¹⁰. The second and third conditions result from simple mass balance: even if NMD anomalies are generated in the atmosphere, isotopically complementary sulphur pools must be removed from the atmosphere and transported to marine sediments with minimal homogenization by inorganic or biological processes. Under these conditions, photochemically derived sulphur containing NMD isotope anomalies will be delivered to the hydrosphere and ultimately buried as a constituent of various sulphur-bearing mineral phases, primarily pyrite (FeS₂). The presence of these anomalies to varying degrees between ~3.8 Gyr ago,

the time of the earliest sedimentary record, and ~2.32 Gyr ago is interpreted to reflect a strongly reducing atmosphere over this entire interval, with the implication that atmospheric p_{O_2} was extremely low for more than half of Earth's history (Fig. 1a). Implicit in this framework is the notion that the generation and transfer of these anomalies into the upper crust through the burial of authigenic marine minerals provides an effectively instantaneous record of ambient atmospheric chemistry, but this assumption ignores the potential importance of sedimentary recycling.

There is a striking asymmetry in the $\Delta^{33}S$ record through Archaean time (Fig. 1a, b), with the data skewed in favour of positive $\Delta^{33}S$ values. Importantly, it is the preservation (and associated crustal recycling) of this NMD sulphur isotope asymmetry that allows for the possibility of a temporal lag between the generation and the ultimate removal of the signal from the oceanic sulphur reservoir. We emphasize that although there are probably several mechanistic explanations for this pattern^{11–13} (Supplementary Information), what matters foremost for our purposes is the veracity of this empirical observation, regardless of mechanism. This observed asymmetry could be misleading if a sedimentary sulphate reservoir with a complementary negative isotopic composition were deposited synchronous with the generation of the record shown in Fig. 1 but has not been preserved through geologic time as a consequence of more rapid weathering, or if seawater sulphate with the negative $\Delta^{33}S$ complement was thermochemically or microbially reduced and buried into a weatherable sedimentary sulphide reservoir that has been strongly undersampled. In the first case, analysis of the more abundant sulphur isotopes (³⁴S and ³²S) indicates that essentially all sulphur entering the Earth surface system was removed as a constituent of pyrite during the Archaean eon¹⁴, leaving little scope for an isotopically complementary Archaean sulphate reservoir that has left no trace on the modern Earth. Consistent with this, extremely low seawater sulphate concentrations during the Archaean relative to the present¹⁵ would probably have rendered large-scale evaporite formation and burial extremely difficult. In the second case, the cumulative average for published $\Delta^{33}S$ values has continued to point to a predominance of positive values in bulk rock measurements as the database of Archaean rare sulphur isotopes has increased in size, while the confidence interval around the mean has continually decreased (Fig. 1b). This relationship indicates that the asymmetry towards positive values does not reflect a sampling bias.

To explore the implications of this asymmetry for long-term recycling of NMD sulphur isotope anomalies, we used a well-established numerical modelling approach. The specific goal was to quantify the importance of recycling $\Delta^{33}S$ signals between the ocean and upper crust (Fig. 2). The model begins with a variation on a class of simple box models used to describe the surface cycling of carbon and sulphur during the Phanerozoic eon, termed 'rapid recycling' models^{16–18}. This group of models and our specific approach are variants on models for global carbon–sulphur–oxygen cycling that have been used for decades to explore the dynamics of these coupled biogeochemical cycles at Earth's surface^{19,20}. Such models have been used extensively to predict

¹Division of Geological and Planetary Sciences, California Institute of Technology, Pasadena, California 91126, USA. ²Department of Earth Sciences, University of California – Riverside, Riverside, California 92521, USA.

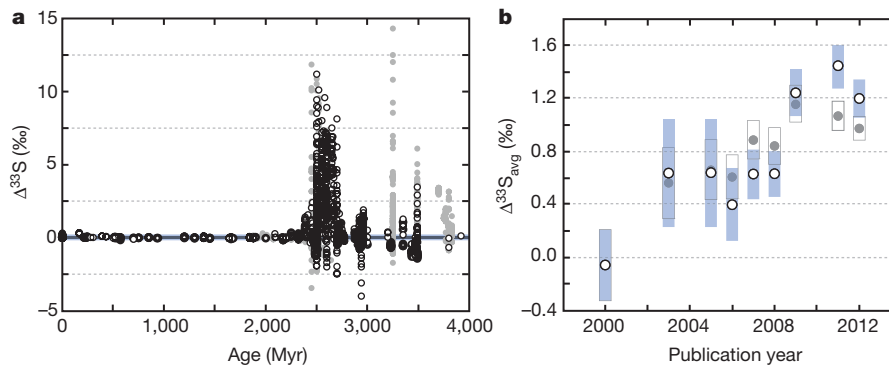


Figure 1 | The rare sulphur isotope record through time. **a**, Data for sedimentary sulphate and sulphide minerals, cast as $\Delta^{33}\text{S}$ (where $\Delta^{33}\text{S} = \delta^{33}\text{S} - 0.515\delta^{34}\text{S}$) versus time. The shaded box ($0.06 \pm 0.16\text{‰}$) denotes the average ± 2 s.d. of all data from within the past 2,200 Myr. Grey points are data generated through secondary ion mass spectrometry (SIMS), and open circles are bulk rock values. **b**, The cumulative average $\Delta^{33}\text{S}$ anomaly as a function of database age for Archaean and early Palaeoproterozoic samples.

atmospheric O_2 and CO_2 concentrations that compare well with independent proxy reconstructions of atmospheric composition during the Phanerozoic^{21,22}. Our model, which tracks only sulphur, partitions sulphur into three reservoirs: the oceanic sulphate pool and two crustal reservoirs of sedimentary pyrite (Fig. 2). The two crustal reservoirs are referred to as ‘young’ and ‘old’, and the primary difference between them other than their overall mass is the speed at which they are recycled. The models build from the geologically reasonable premise that the most recently deposited sediments are more likely to be recycled on a short timescale. Fluxes between reservoirs are predominantly first order with respect to mass; their magnitude depends on the size of the reservoir from which the flux is derived. Three notable exceptions are volcanic inputs and the weathering of igneous (and, thus, isotopically normal, with $\Delta^{33}\text{S} \approx 0\text{‰}$) sulphides, which are both imposed as constant fluxes within a given model run, and the flux between the two crustal pyrite reservoirs. The latter is set equal to the weathering flux from the old pyrite reservoir such that the mass of this reservoir does not change¹⁶.

Our main interest here is tracking the $\Delta^{33}\text{S}$ of seawater sulphate, because this signal will be directly incorporated into sedimentary sulphide minerals under the logical assumption that all subsequent isotope fractionations are mass dependent. We note, however, that there was likely to have been spatial isotopic heterogeneity within the ocean if marine sulphate concentrations were very low, and this possibility has not been incorporated into our model. However, the

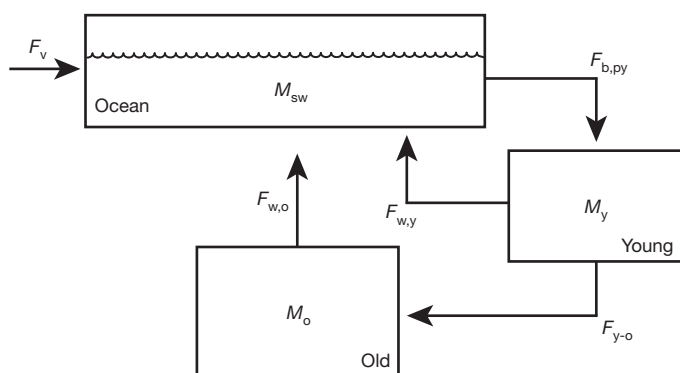


Figure 2 | Schematic diagram of the sulphur isotope mass balance model. Arrows denote flux terms (F_i , where in addition to fluxes already described, $F_{\text{y,o}}$ represents the aging flux of the young crustal reservoir), whereas boxes denote various oceanic and crustal sulphur reservoirs (M_{sw} , M_{y} and M_{o} are the sizes of the seawater reservoir and the two crustal reservoirs, respectively) (Methods Summary).

primary result of spatial isotopic heterogeneity would be to introduce scatter around the trends presented here. In effect, the NMD sulphur isotope signal behaves as a conservative tracer when cycled through a purely mass-dependent sulphur cycle at Earth’s surface. In our model, the isotopic composition of seawater sulphate, $\delta_{\text{sw}}^{33}\text{S}$, will evolve through time according to (Methods and Supplementary Information)

$$M_{\text{sw}} \frac{d\delta_{\text{sw}}^{33}\text{S}}{dt} = \sum_i [F_i(\delta_i^{33}\text{S} - \delta_{\text{sw}}^{33}\text{S})] - F_{\text{b,py}} \Delta_{\text{py}}^{33}\text{S} \quad (1)$$

where M_{sw} is the oceanic mass of seawater sulphate, F_i and $\delta_i^{33}\text{S}$ are respectively the input flux to the ocean and the isotopic composition of reservoir i (from weathering and volcanic sources), $F_{\text{b,py}}$ denotes the pyrite burial flux, $\Delta_{\text{py}}^{33}\text{S}$ denotes the isotopic fractionation between seawater sulphate and sedimentary pyrite, and $x = 3, 4$ or 6 .

The model tracks all four stable sulphur isotopes and includes a parameterization of biologically induced isotope fractionation, but we restrict our attention here to the $\Delta^{33}\text{S}$ composition of sedimentary pyrite formed from chemical or microbial reduction of seawater sulphate, which is derived primarily from the weathering of pyrite. To illustrate most clearly the importance of the sedimentary recycling of $\Delta^{33}\text{S}$ signals, we assume at the beginning of each model run that atmospheric p_{O_2} increases instantaneously above values that allow for the generation and preservation of new NMD sulphur anomalies. All isotope fractionations imposed thereafter are mass dependent and are controlled by metabolic fractionation during microbial sulphate reduction, which is parameterized as a function of ambient seawater sulphate concentration (Supplementary Information). For the purposes of illustration, our simulations are initialized with a $\Delta^{33}\text{S}$ value for seawater sulphate of -1.0‰ (consistent in sign with expectations from photochemical experiments² and analyses of Archaean sulphates^{1,23,24} and seafloor sulphide minerals^{9,23}), although we emphasize that for many periods of Archaean time this value was considerably more negative (Fig. 1a). We then study the effect of various values for the initial $\Delta^{33}\text{S}$ of rapidly weathering sedimentary pyrite, isotopically normal input fluxes (volcanic and igneous weathering) and seawater sulphate concentrations. We stress, however, that these values and the parameter space explored, although certainly plausible, are only meant to be delineative. Our goal is to investigate the timescales on which crustal recycling of NMD isotope anomalies can be expected to leave an imprint on the isotopic composition of the oceanic sulphate reservoir, rather than to simulate specific features of the sedimentary NMD sulphur record. The latter goal is a subject for future research.

There is a notable ‘memory effect’ associated with the sedimentary recycling of $\Delta^{33}\text{S}$ anomalies (Fig. 3a–d), and this memory effect

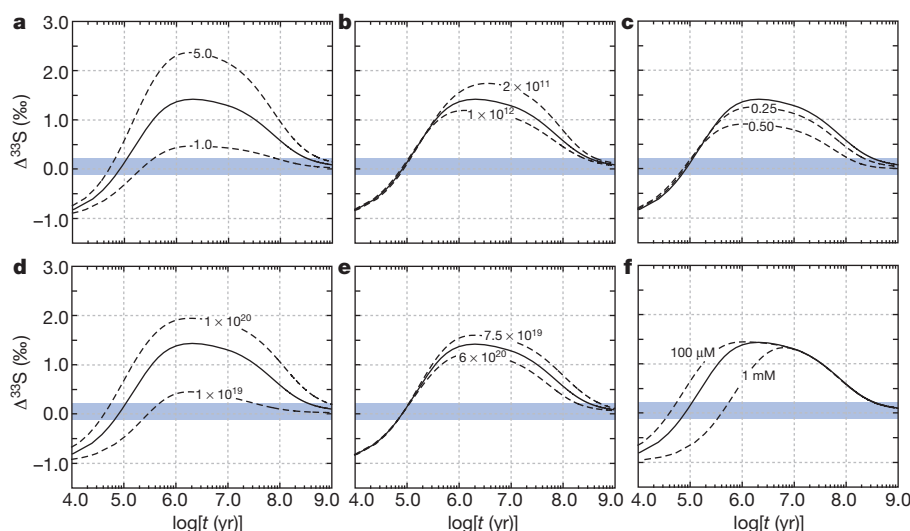


Figure 3 | Modelled changes to the $\Delta^{33}\text{S}$ value of seawater sulphate after the onset of oxidative sulphur cycling. The black solid curve in all cases represents the reference model (Supplementary Information). Dashed curves represent sensitivity analyses as follows: increasing and decreasing the $\Delta^{33}\text{S}$ of the rapidly weathering pyrite reservoir by 2‰ (a); a range of volcanic sulphur fluxes between $2 \times 10^{11} \text{ mol yr}^{-1}$ and $1 \times 10^{12} \text{ mol yr}^{-1}$ (b); increasing the fractional contribution of igneous sulphide weathering to total weathering (c) (values approaching or exceeding 0.5 are considered extremely unlikely; see

Supplementary Information); increasing and decreasing, by factors of 2 and 5, respectively, the initial size of the rapidly weathering pyrite reservoir (d); increasing and decreasing, by factors of 2 and 5, respectively, the size of the slowly weathering pyrite reservoir (e); varying initial oceanic sulphate concentration between 100 μM and 1 mM (f). The shaded box denotes the average ± 2 s.d. of all data from within the past 2,200 Myr. Note that time is displayed on a logarithmic scale.

is difficult to avoid in the parameter space that we consider reasonable. For example, a sizable decrease in the magnitude of residual $\Delta^{33}\text{S}$ values can be achieved by decreasing by a factor of five the size of the rapidly weathering pyrite reservoir from that in the reference model (Fig. 3d). However, this results in geologically unrealistic fluxes and residence times relative to observed mass-age and area-age distributions of weatherable sedimentary rocks^{25,26} and the timescales of cycling through the Earth surface sulphur reservoir²⁷. In other words, this decrease would require a severe departure from the sedimentary rock cycle that has been in place for most of Earth's history (Supplementary Information). Similarly, large, mass-dependent sulphur fluxes from volcanic or igneous sources can in principle dilute the memory effect, but extreme values for these fluxes are required for pronounced attenuation of the residual isotopic signal (Fig. 3b, c). Once NMD isotope fractionations have been introduced into the system in an asymmetric fashion, the best taphonomic conditions for their preservation, in fact, result from all isotope fractionations being mass dependent. This mass dependence prevents homogenization, either locally or on a broad spatial scale, through mixing with isotopically complementary pools.

A residual NMD isotope signal incorporated into sedimentary rocks can persist in our model for roughly 10^8 yr after the cessation of its atmospheric production. However, it is difficult to extend the memory effect beyond the order of a single Wilson cycle (that is, ~ 200 – 250 Myr; Fig. 3). We note, however, that our simple model does not account for time-dependent changes in volcanic sulphur fluxes and microbial processing, and that large perturbations to either of these parameters during the pulsed decay of a residual NMD signal could in principle shorten this timescale somewhat. In addition, the texture, or temporal pattern, of the signal decay (regardless of the ultimate timescale of the memory effect) will depend strongly on the initial $\Delta^{33}\text{S}$ value and the initial size of the seawater sulphate reservoir (Fig. 3a, f). Larger seawater sulphate concentrations will result in greater temporal inertia as the system moves towards the isotopic properties of the weathering input with positive $\Delta^{33}\text{S}$ values.

An important outcome of this dynamic within the residual isotopic signal is that oscillations in atmospheric p_{O_2} near or well above the threshold for the generation and synchronous preservation of NMD isotope anomalies may be expected to produce a wide range of

temporal responses depending on the speed and periodicity of the oscillation. Most of the texture during each simulation is centred on the 10^5 – 10^7 -yr timescale, during which the $\Delta^{33}\text{S}$ values of seawater sulphate in the model will change from being strongly negative to being strongly positive (Fig. 3). In addition, during periods of NMD sulphur production the $\Delta^{33}\text{S}$ composition of sea water should rapidly change back to values governed by atmospheric sulphur input, on a timescale ultimately dependent on the size of the seawater sulphate reservoir but probably not greatly in excess of $\sim 10^5$ yr. The net result of this would be an extremely dynamic, perhaps even noisy, rare sulphur isotope record, despite extremely long periods of oxidative crustal weathering.

It is commonly argued that biological oxygen production preceded the broad-scale and effectively permanent accumulation of oxygen in Earth's atmosphere by perhaps 200 Myr or more^{5–8,28,29}. Consistent with oxygenation before the so-called Great Oxidation Event, some data imply oxidative weathering over this interval^{5–8}. Our model suggests the possibility of excursions in atmospheric O_2 content that may have been well above the upper threshold for generating and preserving NMD sulphur isotope anomalies in marine sediments long before the disappearance of these signals from the record, on timescales more than adequate to support extensive oxidative weathering of crustal minerals^{5,7}. Alternation between periods of generation and non-generation of atmospheric NMD isotope anomalies on a range of timescales (10^5 – 10^8 yr) would not be immediately manifest in the removal of these signals from the rock record due to the recycling effect. It has been suggested that the behaviour of O_2 in a relatively reducing atmosphere is likely to be characterized by strong hysteresis³⁰—such that the attainment of relatively 'high' O_2 (above $\sim 10^{-5}$ times the present atmospheric level) may not be readily undone. Nevertheless, with atmospheric p_{O_2} values (and, thus, residence times) far below those characteristic of the modern Earth we would naturally expect high-frequency oscillations in atmospheric p_{O_2} with corresponding periods much shorter than the duration of the crustal memory effect within the $\Delta^{33}\text{S}$ record, and with biological oxygen production emergent and the interplay between this process and inorganic buffering mechanisms varying in ways that may have been episodic.

The model permits oscillatory behaviour for the oxygen cycle during earlier portions of Archaean time, because NMD signals would persist even as p_{O_2} rose and fell on timescales of millions of years. However,

our model also implies that a pulsed or irreversible rise in atmospheric O₂ during the late Archaean may have preceded the ultimate disappearance of NMD sulphur isotope anomalies from the rock record by ~10⁷–10⁸ yr. Combined, these results suggest that the texture of atmospheric redox evolution on the early Earth may have been highly dynamic and may call into question the notion of a Great Oxidation Event as strictly understood—that is, that there was a moment or brief period in Earth's history when the oxygen concentration increased permanently to levels above those required to support the production and preservation of NMD anomalies in the atmosphere—and instead suggest that the oxygenation of the atmosphere could have been a protracted process⁸. Viewed in this way, our model suggests that many of the climatological and geochemical upheavals witnessed by the Archaean–Proterozoic transition, including the earliest recorded widespread glaciations³¹ and the deposition of perhaps the largest iron and manganese deposits in Earth's history³², may have been linked more directly to excursions in atmospheric O₂ content than current interpretations of the rare sulphur isotope record indicate. The details of oscillatory redox behaviour and the timing of oxygen's irreversible increase, along with the further constraint of the input parameters controlling the fabric and lags in the NMD record, are topics for future research. Nevertheless, recycling of crustal sulphur with relict NMD isotope anomalies must be considered in further attempts to explore quantitatively the palaeoenvironmental and palaeobiological implications of the Archaean sulphur isotope record.

METHODS SUMMARY

We model the dynamics of the isotopic composition of seawater sulphate through time, as governed by the input fluxes and isotopic compositions of sulphur associated with weathering of sulphides from two sedimentary reservoirs ($F_{w,y}$ and $F_{w,o}$), weathering of sulphide from an igneous (and, thus, isotopically normal) reservoir ($F_{w,ig}$) and volcanic sulphur emissions (F_v), balanced against the removal of sulphur from the ocean in association with the burial of sedimentary pyrite ($F_{b,py}$). The time-dependent isotope mass balance equation for seawater sulphate is then given by equation (1). The isotopic composition of a given reservoir i is defined according to conventional 'delta' notation as $\delta_i^{3x} = \left(\frac{{}^{3x}\text{S}/{}^{32}\text{S}}{\text{sample}} / \frac{{}^{3x}\text{S}/{}^{32}\text{S}}{\text{standard}} - 1 \right) \times 10^3\%$, where the standard is defined relative to the isotopic composition of Vienna Canyon Diablo Troilite. A detailed discussion of the model set-up and parameterization, references for the sulphur isotope database and details of compilation and statistical treatment are provided in Methods and Supplementary Information.

Full Methods and any associated references are available in the online version of the paper.

Received 8 August 2012; accepted 19 February 2013.

Published online 24 April 2013.

1. Farquhar, J., Bao, H. & Thiemens, M. Atmospheric influence of Earth's earliest sulfur cycle. *Science* **289**, 756–758 (2000).
2. Farquhar, J., Savarino, J., Airieau, S. & Thiemens, M. H. Observation of wavelength-sensitive mass-independent sulfur isotope effects during SO₂ photolysis: implications for the early atmosphere. *J. Geophys. Res.* **106**, 32829–32839 (2001).
3. Pavlov, A. A. & Kasting, J. F. Mass-independent fractionation of sulfur isotopes in Archean sediments: strong evidence for an anoxic Archean atmosphere. *Astrobiology* **2**, 27–41 (2002).
4. Bekker, A. *et al.* Dating the rise of atmospheric oxygen. *Nature* **427**, 117–120 (2004).
5. Anbar, A. D. *et al.* A whiff of oxygen before the Great Oxidation Event? *Science* **317**, 1903–1906 (2007).
6. Frei, R., Gaucher, C., Poulton, S. W. & Canfield, D. E. Fluctuations in Precambrian atmospheric oxygenation recorded by chromium isotopes. *Nature* **461**, 250–253 (2009).

7. Reinhard, C. T., Raiswell, R., Scott, C., Anbar, A. D. & Lyons, T. W. A late Archean sulfidic sea stimulated by early oxidative weathering of the continents. *Science* **326**, 713–716 (2009).
8. Konhauser, K. O. *et al.* Aerobic bacterial pyrite oxidation and acid rock drainage during the Great Oxidation Event. *Nature* **478**, 369–373 (2011).
9. Ono, S. *et al.* New insights into Archean sulfur cycle from mass-independent sulfur isotope records from the Hamersley Basin, Australia. *Earth Planet. Sci. Lett.* **213**, 15–30 (2003).
10. Halevy, I., Johnston, D. T. & Schrag, D. P. Explaining the structure of the Archean mass-independent sulfur isotope record. *Science* **329**, 204–207 (2010).
11. Farquhar, J. *et al.* Inclusions in diamond and sulfur recycling on early Earth. *Science* **298**, 2369–2372 (2002).
12. Farquhar, J. & Wing, B. A. Multiple sulfur isotopes and the evolution of the atmosphere. *Earth Planet. Sci. Lett.* **213**, 1–13 (2003).
13. Bekker, A. *et al.* Atmospheric sulfur in Archean komatiite-hosted nickel deposits. *Science* **326**, 1086–1089 (2009).
14. Canfield, D. E. & Farquhar, J. Animal evolution, bioturbation, and the sulfate concentration of the oceans. *Proc. Natl Acad. Sci. USA* **106**, 8123–8127 (2009).
15. Habicht, K. S., Gade, M., Thamdrup, B., Berg, P. & Canfield, D. E. Calibration of sulfate levels in the Archean ocean. *Science* **298**, 2372–2374 (2002).
16. Berner, R. A. Models for carbon and sulfur cycles and atmospheric oxygen: application to Paleozoic geologic history. *Am. J. Sci.* **287**, 177–196 (1987).
17. Berner, R. A. & Canfield, D. E. A new model for atmospheric oxygen over Phanerozoic time. *Am. J. Sci.* **289**, 333–361 (1989).
18. Berner, R. A. Modeling atmospheric O₂ over Phanerozoic time. *Geochim. Cosmochim. Acta* **65**, 685–694 (2001).
19. Garrels, R. M. & Lerman, A. Coupling of the sedimentary sulfur and carbon cycles—an improved model. *Am. J. Sci.* **284**, 989–1007 (1984).
20. Kump, L. R. & Garrels, R. M. Modeling atmospheric O₂ in the global sedimentary redox cycle. *Am. J. Sci.* **286**, 337–360 (1986).
21. Royer, D. L., Berner, R. A. & Beerling, D. J. Phanerozoic atmospheric CO₂ change: evaluating geochemical and paleobiological approaches. *Earth Sci. Rev.* **54**, 349–392 (2001).
22. Scott, A. C. & Glasspool, I. J. The diversification of Paleozoic fire systems and fluctuations in atmospheric oxygen concentration. *Proc. Natl Acad. Sci. USA* **103**, 10861–10865 (2006).
23. Farquhar, J. & Wing, B. A. The terrestrial record of stable sulphur isotopes: a review of the implications for evolution of Earth's sulphur cycle. *Spec. Publ. Geol. Soc. (Lond.)* **248**, 167–177 (2005).
24. Ueno, Y., Ono, S., Rumble, D. & Maruyama, S. Quadruple sulfur isotope analysis of ca. 3.5 Ga Dresser Formation: new evidence for microbial sulfate reduction in the early Archean. *Geochim. Cosmochim. Acta* **72**, 5675–5691 (2008).
25. Bluth, G. J. S. & Kump, L. R. Phanerozoic paleogeology. *Am. J. Sci.* **291**, 284–308 (1991).
26. Gregor, C. B. The mass-age distribution of Phanerozoic sediments. *Geol. Soc. Lond. Mem.* **10**, 284–289 (1985).
27. Garrels, R. M. & Mackenzie, F. T. A quantitative model for the sedimentary rock cycle. *Mar. Chem.* **1**, 27–41 (1972).
28. Kaufman, A. J. *et al.* Late Archean biospheric oxygenation and atmospheric evolution. *Science* **317**, 1900–1903 (2007).
29. Garvin, J., Buick, R., Anbar, A. D., Arnold, G. L. & Kaufman, A. J. Isotopic evidence for an aerobic nitrogen cycling in the latest Archean. *Science* **323**, 1045–1048 (2009).
30. Goldblatt, C., Lenton, T. M. & Watson, A. J. Bistability of atmospheric oxygen and the Great Oxidation. *Nature* **443**, 683–686 (2006).
31. Evans, D. A., Beukes, N. J. & Kirschvink, J. L. Low-latitude glaciation in the Palaeoproterozoic era. *Nature* **386**, 262–266 (1997).
32. Maynard, J. B. The chemistry of manganese ores through time: a signal of increasing diversity of Earth-surface environments. *Econ. Geol.* **105**, 535–552 (2010).

Supplementary Information is available in the online version of the paper.

Acknowledgements Funding from NSF-EAR and the NASA Exobiology Program supported this research. C.T.R. acknowledges support from an O. K. Earl Postdoctoral Fellowship in Geological and Planetary Sciences at the California Institute of Technology. N.J.P. acknowledges support from NSF-EAR-PDF. Comments and criticism from L. Kump, B. Wing, A. Bekker and K. Konhauser greatly improved the manuscript.

Author Contributions C.T.R. and N.J.P. designed the model. C.T.R. compiled the sulphur isotope database and performed the modelling and statistical analyses. C.T.R. and N.J.P. wrote the manuscript, with contributions from T.W.L.

Author Information Reprints and permissions information is available at www.nature.com/reprints. The authors declare no competing financial interests. Readers are welcome to comment on the online version of the paper. Correspondence and requests for materials should be addressed to C.T.R. (reinhard@caltech.edu).

METHODS

Model structure. The model consists of three Earth surface sulphur reservoirs: an oceanic sulphate reservoir (M_{sw}) and two crustal sulphur reservoirs (referred to, following refs 16–18, 33, 34, as ‘young’ (M_y) and ‘old’ (M_o)). The distinction between two crustal reservoirs of varying cycling speeds was initially introduced to more directly couple the carbon and sulphur isotope compositions of fluxes out of the ocean to that of fluxes into the ocean, in an effort to alleviate physically unrealistic shifts in atmospheric composition due to changes in measured isotope ratios of sedimentary carbonate and sulphate minerals^{16,33}. However, there is also ample geological justification for such a model configuration^{16–18,27,33–35}, and subsequent work has shown that this assumption results in a good agreement between proxy-based reconstructions of Phanerozoic atmospheric composition and those derived from mass balance models^{21,22,34,36,37}.

Model equations. Full derivation of the mass balance equations is given in Supplementary Information. The model solves a series of coupled isotope mass balance equations for oceanic and crustal sulphur:

$$M_{sw} \frac{d\delta_{sw}^{3x}}{dt} = \sum_i [F_i(\delta_i^{3x} - \delta_{sw}^{3x})] - F_{b,py} \Delta_{py}^{3x}$$

$$M_y \frac{d\delta_y^{3x}}{dt} = F_{b,py}(\delta_{py}^{3x} - \delta_y^{3x})$$

$$M_o \frac{d\delta_o^{3x}}{dt} = F_{y-o}(\delta_y^{3x} - \delta_o^{3x})$$

where F terms denote sulphur fluxes and M terms refer to reservoir sizes. The δ terms denote sulphur isotope compositions of the different reservoirs and fluxes according to conventional ‘delta’ notation, $\delta_i^{3x} = \left(\frac{(^{3x}\text{S}/^{32}\text{S})_{\text{sample}}}{(^{3x}\text{S}/^{32}\text{S})_{\text{standard}}} - 1 \right) \times 10^3\%$, where the standard is defined relative to the isotopic composition of Vienna Canyon Diablo Troilite, and $x = 3, 4$ or 6 . The Δ term in the first equation describes the metabolic fractionation imparted by dissimilatory sulphate reduction as expressed on a global scale, and is described by a Monod-type function (Supplementary Information).

Initial parameterization. Model parameters for our reference case are shown in Supplementary Table 1. Parameter values for the reference case were chosen to approximately satisfy known constraints on the overall size of the crustal sulphur reservoir^{16,19,38,39}, the residence time of sulphur as it cycles through the exogenic system^{20,27}, the fraction of overall sulphur input derived from the rapidly recycling sulphur reservoir^{25,34,40–42}, the residence time of sulphur in the rapidly recycling reservoir with respect to weathering^{16,17}, and the residence time of sulphur in the rapidly recycling reservoir with respect to removal to the old reservoir^{16,34,42} (the ‘aging flux’ of the young pyrite reservoir). The range of F_y values was chosen to encompass estimates of the modern volcanic sulphur flux and values scaled up to reflect the possibility of greater crustal heat flow and volcanic activity during Earth’s early history. Estimates of the modern volcanic sulphur flux are typically of the order of $\sim(2-3) \times 10^{11} \text{ mol yr}^{-1}$ (refs 39, 43–47), and we use an estimate of $2 \times 10^{11} \text{ mol yr}^{-1}$ as our low volcanic flux. Heat flow through the crust has decreased with time, and as a result it is typically assumed that Earth’s early history

was characterized by increased rates of volcanism. Estimates vary, but it is unlikely that crustal heat flow during the Archaean was more than $\sim 3-4$ times that of the modern Earth^{48–51}. We therefore use a volcanic sulphur input of $1 \times 10^{12} \text{ mol yr}^{-1}$ as our high volcanic flux. We note, however, that higher rates of heat flow through the crust need not require an increase in the mass flux from subaerial volcanic activity—much of this heat loss may have been accommodated by submarine mafic spreading centres⁵², which are essentially sulphur neutral in an anoxic and iron-buffered deep ocean. In each model run, the pyrite burial rate constant (k_{py}) is solved for to attain a steady state with the prescribed volcanic sulphur flux. Oxidative weathering of sedimentary and igneous rocks is then initialized, and the model allowed to evolve freely.

33. Berner, R. A. Biogeochemical cycles of carbon and sulfur and their effect on atmospheric oxygen over Phanerozoic time. *Palaeogeogr. Palaeoclimatol. Palaeoecol.* **75**, 97–122 (1989).
34. Berner, R. A. GEOCARBSULF: a combined model for Phanerozoic atmospheric O₂ and CO₂. *Geochim. Cosmochim. Acta* **70**, 5653–5664 (2006).
35. Garrels, R. M. & Mackenzie, F. T. Sedimentary rock types: relative proportions as a function of geological time. *Science* **163**, 570–571 (1969).
36. Royer, D. L., Berner, R. A., & Park, J. Climate sensitivity constrained by CO₂ concentrations over the past 420 million years. *Nature* **446**, 530–532 (2007).
37. Berner, R. A. & Kothavala, Z. GEOCARB III: a revised model of atmospheric CO₂ over Phanerozoic time. *Am. J. Sci.* **301**, 182–204 (2001).
38. Li, Y.-H. Geochemical mass balance among lithosphere, hydrosphere, and atmosphere. *Am. J. Sci.* **272**, 119–137 (1972).
39. Canfield, D. E. The evolution of the Earth surface sulfur reservoir. *Am. J. Sci.* **304**, 839–861 (2004).
40. Garrels, R. M., Lerman, A. & Mackenzie, F. T. Controls of atmospheric O₂ and CO₂: past, present, and future. *Am. Sci.* **64**, 306–315 (1976).
41. Blatt, H. & Jones, R. L. Proportions of exposed igneous, metamorphic, and sedimentary rocks. *Geol. Soc. Am. Bull.* **86**, 1085–1088 (1975).
42. Berner, R. A. A model for atmospheric CO₂ over Phanerozoic time. *Am. J. Sci.* **291**, 339–376 (1991).
43. Berresheim, H. & Jaeschke, W. The contribution of volcanoes to the global atmospheric sulfur budget. *J. Geophys. Res.* **88**, 3732–3740 (1983).
44. Walker, J. C. G. & Brimblecombe, P. Iron and sulfur in the pre-biologic ocean. *Precamb. Res.* **28**, 205–222 (1985).
45. Andres, R. J. & Kasgnoc, A. D. A time-averaged inventory of subaerial volcanic sulfur emissions. *J. Geophys. Res.* **103**, 25251–25261 (1998).
46. Halmer, M. M., Schmincke, H.-U. & Graf, H.-F. The annual volcanic gas input into the atmosphere, in particular to the stratosphere: a global data set for the past 100 years. *J. Volcanol. Geotherm. Res.* **115**, 511–528 (2002).
47. Canfield, D. E., Rosing, M. T. & Bjerrum, C. Early anaerobic metabolisms. *Phil. Trans. R. Soc. B* **361**, 1819–1836 (2006).
48. Schubert, G., Stevenson, D. & Cassen, P. Whole planet cooling and the radiogenic heat source contents of the Earth and Moon. *J. Geophys. Res.* **85**, 2531–2538 (1980).
49. Christensen, U. R. Thermal evolution models for the Earth. *J. Geophys. Res.* **90**, 2995–3007 (1985).
50. Lenardic, A. Continental growth and the Archaean paradox. *Geophys. Monogr. Ser.* **164**, 33–45 (2006).
51. Padhi, C. M., Korenaga, J. & Ozima, M. Thermal evolution of Earth with xenon degassing: a self-consistent approach. *Earth Planet. Sci. Lett.* **341–344**, 1–9 (2012).
52. Kump, L. R. & Barley, M. E. Increased subaerial volcanism and the rise of atmospheric oxygen 2.5 billion years ago. *Nature* **448**, 1033–1036 (2007).